Mean-field models of size selection in polymer vesicles with and without interdigitation

M. J. Greenall[a]* and H. J. Macpherson[a]

[a]*School of Mathematics and Physics, University of Lincoln, Lincoln, LN6 7TS, United Kingdom*

*School of Mathematics and Physics, University of Lincoln, Lincoln, LN6 7TS, United Kingdom

Mean-field models of size selection in polymer vesicles with and without interdigitation

Block copolymers in solution can form vesicles with a preferred size when the degree of polymerisation N_B of the hydrophobic block is significantly greater than that of the hydrophilic block. In an earlier publication, we introduced a mean-field theory that treats the vesicle membrane as a bilayer. Here, a model is presented in which the hydrophobic blocks form a single interdigitated layer. In the model with interdigitation, the vesicles still have a preferred radius, but this increases more slowly as a function of N_B than in the bilayer model, in better agreement with experiment. However, the predictions of the bilayer model for the relationship between N_B and the vesicle membrane thickness T_m are consistent with the experimental result $T_m \propto N_B^{0.79}$ over a wide range of parameters, while the model with interdigitation predicts an exponent of around $2/3$. This suggests that the structure of the vesicles may lie between these two cases.

Keywords: polymers; vesicles; amphiphiles; self-assembly

Introduction

Amphiphilic molecules such as block copolymers can self-assemble into various structures in solution [1]. An example of such a structure is the *vesicle*, a bag-like membrane that encloses a volume of solvent. Controlling the size of vesicles is of interest, as these aggregates can be used to encapsulate and deliver drugs [2], and the size of a vesicle determines the dosage it contains. However, this is a difficult problem [3], since there is not always a direct link between the size of a vesicle and the architecture of the polymers of which it is formed. The factor that determines the size of vesicles formed by self-assembly in solution is commonly their translational entropy [4, 5]. Although it restricts the size of vesicles, this effect does not lead to precise control over their radius [6, 7], which also depends strongly on the concentration of amphiphiles [8]. Control over vesicle size is often gained in practice by using mechanical methods such as filtration [9] or de-wetting from a patterned surface [10]. It is also possible to induce a preferred curvature in a vesicle membrane, thereby fixing its size, by mixing two types of amphiphile [11] or by using copolymers with several sections [3]. Unfortunately, these final two methods introduce their own complications, with structures other

than vesicles forming when two amphiphiles are mixed and more sophisticated synthesis being necessary to form complex copolymers [3].

However, in experiments carried out by Warren et al [12], vesicles with a small range of sizes have been formed by self-assembly in a solution of only one species of diblock copolymer. In this work, vesicles with very similar size distributions were made by two different methods: polymerisation-induced self-assembly (PISA), where the hydrophobic block continues to grow as the self-assembly takes place, and rehydration of a film of copolymer [12]. This implies that the equilibrium phase in this system may be a suspension of vesicles with a narrow size distribution. The distinguishing feature of the polymers that form these vesicles is that they are highly asymmetric, with the hydrophobic block containing as many as 15 times more repeat units than the hydrophilic block [12].

In an earlier publication [13], we reported a simple mean-field model that reproduced several aspects of these experimental systems. The model contained a free-energy minimum that corresponded to a preferred size for the vesicles, and this minimum appeared when the hydrophobic block of the copolymers was significantly longer than the hydrophilic block. The instability of the vesicles at very high block asymmetries seen in the above experiments was also reproduced by the model. An assumption of this theory was that the vesicle membrane consisted of a bilayer, that is, two distinct layers of molecules (see Fig. 1). However, this is not the only possibility [14] and it has been found in both experiments [15] and simulations [16] that long copolymers can form an *interdigitated* structure in which the hydrophobic blocks of the inner and outer layers of the membrane interpenetrate (see Fig. 2). In this report, we present a model including interdigitation. Our first motivation is to show that the prediction of a preferred size for the vesicles is not an artefact of assuming the existence of two bilayers and our second is to compare the predictions of the two models to attempt to see which physical picture is more appropriate.

Mean-field model with interdigitation

Mean-field models have been employed to investigate the self-assembly of micelles [17–20] and of flat bilayers [21]. These theories agree quite well with experiments on micelle formation in both blends of block copolymers with homopolymers [22] and in

solutions of block copolymers [23]. They are computationally much less expensive than alternative methods such as coarse-grained simulations [16], making them a useful tool for preliminary investigations of a system. To construct a mean-field model for amphiphile self-assembly, assumptions are made for the main contributions to the free energy of a system of aggregates. Examples of effects that are typically included are [17] the free energy costs associated with forming an interface at the boundary of the core of an aggregate and with deforming the copolymers with respect to their unperturbed state.

The various terms in the free energy are then summed, and the resulting function is minimised, giving predictions for a range of quantities, such as the number of molecules in each aggregate. Here, this approach is used to study a suspension of spherical vesicles. Given that the aim of this work is to capture the basic physics of the system and allow a more detailed model to be developed in the future, the theory is formulated for a simple system in which the copolymers that form the vesicles consist of N_A A monomers and N_B B monomers and are dispersed in homopolymers each containing N_h A monomers.

The first contributions to the free energy to be introduced are those for a single vesicle. As referred to above, there will be a term that models the deformation of the copolymer molecules [17]. Following the approach of [17, 24] and including both the polymers whose hydrophilic blocks constitute the outer layer of the vesicle (see Fig. 2) and those whose hydrophilic blocks constitute the inner layer, we have

$$\mathcal{F}_d = \frac{3}{2}kT\left\{p_1\left[\frac{(R_1-R_0)^2}{N_A a^2}+\frac{N_A a^2}{(R_1-R_0)^2}+\frac{(R_2-R_1)^2}{N_B a^2}+\frac{N_B a^2}{(R_2-R_1)^2}-4\right]\right.$$
$$\left.+\,p_2\left[\frac{(R_2-R_1)^2}{N_A a^2}+\frac{N_A a^2}{(R_2-R_1)^2}+\frac{(R_3-R_2)^2}{N_B a^2}+\frac{N_B a^2}{(R_3-R_2)^2}-4\right]\right\} \quad (1)$$

where k is Boltzmann's constant, T is the temperature, a is the segment length, p_1 is the number of copolymers whose hydrophilic blocks point towards the centre of the vesicle, p_2 is the number whose hydrophilic blocks point outwards and the R_i are the radii shown in Fig. 2. When the molecules are in their unperturbed state, the numerator of each term becomes equal to the corresponding denominator and the expression overall is zero. Correspondingly, an energy penalty is given when the copolymers are stretched or compressed away from their unperturbed state. It should be noted that this is a very simple model for chain stretching, and more sophisticated theories are available, such as the strong-stretching models reviewed in [25]. However, use of these approaches would

require more detail in several aspects of the current model, in particular the position dependence of the various volume fractions. Here, our goal is to capture the basic phenomenology and scaling of this system in as simple a theory as possible, and, as will be discussed in the final section, we believe that a more promising next step would be to move directly to a more microscopic model such as self-consistent field theory [26] rather than refining individual terms in the current model.

It is assumed that the hydrophilic layers of the vesicle (light grey in Fig. 2) are composed of copolymer A blocks mixed with solvent, and the hydrophobic layers (dark grey in Fig. 2) of copolymer B blocks mixed with solvent. A term is therefore included that models the entropy of mixing of the copolymer chains with the solvent [17]. For the vesicle shown in Fig. 2, this is

$$\mathcal{F}_m = \sum_{i=1}^{3} \frac{4\pi}{3} \frac{R_i^3 - R_{i-1}^3}{a^3} kT \frac{1-\eta_i}{N_h} \ln(1-\eta_i), \qquad (2)$$

where the volume fraction of copolymer in each layer is η_i. Since the vesicle has three layers, the index i runs from 1 to 3. The volume fraction in the central layer η_2 is allowed to take values less than one in order to model the ingress of water into the vesicle membrane seen in the experiments of Warren et al [12].

The solvent that penetrates into the central layer of the vesicle membrane has a repulsive interaction with the hydrophobic blocks in this region. This is modelled by [23] the following term in the free energy:

$$\mathcal{F}_{\text{core}} = \frac{4\pi}{3} \frac{(R_2^3 - R_1^3)}{a^3} kT\eta_2(1-\eta_2)\chi, \qquad (3)$$

where χ is the Flory-Huggins parameter that determines the strength of the interaction.

Within the vesicle membrane, there are two surfaces that divide a hydrophilic layer from the mainly hydrophobic central layer. Each of these surfaces gives a contribution to the vesicle free energy [17, 27] that is proportional to its area and to $\sqrt{\chi}$. Since the central layer contains some solvent [23], the surface free energy is lower than it would be for an interface between a purely hydrophobic and a purely hydrophilic layer. This can be modelled [23] by including an extra factor of η_2, yielding

$$\mathcal{F}_{int} = 4\pi R_1^2 \frac{kT}{a^2}\sqrt{\frac{\chi}{6}}\eta_2 + 4\pi R_2^2 \frac{kT}{a^2}\sqrt{\frac{\chi}{6}}\eta_2. \qquad (4)$$

The total free energy of a single vesicle can now be calculated by summing the terms introduced above: $\mathcal{F} = \mathcal{F}_d + \mathcal{F}_m + \mathcal{F}_{int}$. It is also assumed that the system is incompressible. This allows the volume fractions in a given layer η_i to be expressed in

terms of the dimensions of that layer, the number of copolymers in it and the degree of polymerisation of the relevant block. For example, in layer 1, $\eta_1 = 3p_1N_Aa^3/[4\pi(R_1^3 - R_0^3)]$.

The first step in calculating the free energy of a system of vesicles is to find an expression for the number of vesicles. If Ω is the total number of monomers in the system (including both copolymers and solvent), ϕ is the volume fraction of copolymers and ζ is the fraction of copolymer chains in vesicles, then the total number of vesicles is found by dividing the total number of monomers in vesicles, $\Omega\phi\zeta$, by the number of monomers in one vesicle, giving $\Omega\phi\zeta/[(p_1 + p_2)(N_A + N_B)]$. The total free energy of the system can then be written as

$$F_M = \{\Omega\phi\zeta/[(p_1 + p_2)(N_A + N_B)]\}\mathcal{F} + F_{\text{mix}} - TS_m, \qquad (5)$$

The final two terms are the free energy of mixing of solvent and copolymers outside the vesicles [28] and the translational entropy of the vesicles [17] respectively. As in [13], the first of these is given by

$$\frac{F_{\text{mix}}}{kT} = \Omega(1 - \xi\phi\zeta)\left[\frac{\phi_1}{N_A + N_B}\ln\phi_1 + \frac{1 - \phi_1}{N_h}\ln(1 - \phi_1) + \frac{\chi N_B\phi_1}{N_A + N_B}\left(1 - \frac{\phi_1 N_B}{N_A + N_B}\right)\right], \qquad (6)$$

where $\Omega(1 - \xi\phi\zeta)$ is the total number of monomers outside the vesicles and $\phi_1 = \phi(1 - \zeta)/(1 - \xi\phi\zeta)$ is the fraction of monomers outside vesicles that belong to copolymers. However, since the vesicle now consists of three layers with both outward- and inward-pointing polymers in the central layer, the quantity ξ is now given by

$$\xi = \frac{1}{(p_1 + p_2)(N_A + N_B)}\left(\frac{p_1N_A}{\eta_1} + \frac{(p_1 + p_2)N_B}{\eta_2} + \frac{p_2N_A}{\eta_3}\right). \qquad (7)$$

Again as in [13], the translational entropy of micelles is

$$\frac{S_m}{k} = -\Omega\left\{\frac{\phi\zeta}{(p_1 + p_2)(N_A + N_B)}\ln\left(\phi\zeta\tilde{\xi}\right) + \frac{1 - \phi\zeta\tilde{\xi}}{\tilde{\xi}(p_1 + p_2)(N_A + N_B)}\ln\left(1 - \phi\zeta\tilde{\xi}\right)\right\}, \qquad (8)$$

but with $\tilde{\xi}$ now modified to $\tilde{\xi} = 4\pi R_3^3/[(p_1 + p_2)(N_A + N_B)3a^3]$ since the outer radius in the model with interdigitation is R_3 rather than R_4.

In each numerical calculation, N_A, N_B, χ and the outer radius R_3 are fixed and the free energy in Eqn. (5) is minimised with a direction set approach [29] with respect to R_0, R_1, R_2, p_1, p_2 and ϕ_1. This calculation is then repeated for a range of values of R_3, allowing the free energy to be plotted as a function of the outer radius. If this graph has a minimum, the value of R_3 at this point will give the preferred radius of the vesicle.

Results

To make a direct comparison with the results of [13], the same values for the fixed polymer degrees of polymerisation are chosen ($N_A = 100$, $N_h = 1$). The values of the copolymer volume fraction ($\phi = 0.01$) and the Flory-Huggins interaction parameter ($\chi = 2$) are also set to the values used in this earlier paper. Choosing $\phi = 0.01$ gives a dilute system in which the interactions of the vesicles may be neglected. The relatively high value of χ was chosen in [13] to make sure that aggregation occurs for a range of values of N_B. It will be seen later that, for all systems in the interdigitated model and most systems in the bilayer model, lowering this parameter to $\chi = 1$ (more typical of hydrophobic block-solvent interactions [30]) does not strongly affect the results. Plots of $F_M/\Omega kT$ as a function of N_B with the other parameters set to the values above are shown in Fig. 3. As in the case of the bilayer model, we find a minimum in the free energy as a function of R_3 for certain values of N_B, showing that the prediction of a preferred size for the vesicles is not an artefact of the bilayer assumption. This minimum first appears at $N_B \approx 400$ (Fig. 3(a)) and moves outwards as N_B is increased, remaining present until around $N_B \approx 900$ (Fig. 3(c)). This range is much broader than for the corresponding polymers in the bilayer model, where the vesicle is only stable between $N_B \approx 380$ and $N_B \approx 440$. As in the case of the bilayer model, the minimum vanishes (Fig. 3(d)) as the degree of polymerisation of the hydrophobic block is increased beyond a critical value (here, $N_B \approx 1000$) and the vesicle morphology becomes unstable.

To continue the comparison of the models with and without interdigitation, we now consider longer copolymers with N_A set to 1000 and N_B allowed to vary (Fig. 4). The other parameters are set as above. In these systems, clear minima in the free energy are found for a range of values of N_B. As for $N_A = 100$, this minimum is present for a wider range of values of N_B in the model with interdigitation than in the bilayer model. In Fig. 4(a), where $N_B = 7000$, the minimum is just visible; in Fig. 4(c), where $N_B = 29000$, it is still apparent but has moved to a much larger value of R_3. When $N_B = 32000$ (Fig. 4(d)), the preferred radius is no longer present. The value of N_B at which the vesicle becomes unstable is significantly higher than than that ($N_B \approx 17500$) in the bilayer model.

The basic phenomenology is similar in both models: vesicles with an optimum size are stable when the polymers are sufficiently asymmetric ($N_B \gg N_A$) and become

unstable when the degree of polymerisation of the hydrophobic block increases beyond a critical value. To compare the models in more detail, we now plot the outer radius of the vesicle against the degree of polymerisation N_B of the hydrophobic block for $N_A = 100$ (Fig. 5(a)) and $N_A = 1000$ (Fig. 5(b)). In both cases, the outer radius grows more slowly as a function of N_B in the interdigitated model than in the bilayer model and, as noted earlier, the vesicles remain stable over a wider range of N_B when interdigitation is included. Arguably, this slow growth is in better agreement with experimental results [12], where the outer radius of the vesicles remains close to constant as N_B is increased.

To make a quantitative comparison between the two models, the dependence of the membrane thickness T_m on N_B is calculated for each model for a range of values of hydrophilic block degrees of polymerisation N_A. For each value of N_A, T_m vs. N_B is plotted over the full range of N_B for which the vesicles are stable. T_m is defined as the thickness of the hydrophobic layer [12] and is given by $R_2 - R_1$ in the model with interdigitation and by $R_3 - R_1$ in the bilayer model. Fig. 6 shows log-log plots of T_m as a function of N_B for a range of hydrophilic block degrees of polymerisation from $N_A = 100$ to $N_A = 1500$. Each panel shows results from $\chi = 1$ (lowest curve) to $\chi = 3$ (uppermost curve) with χ increasing in steps of 0.5. All curves are close to being power laws with an exponent of approximately $2/3$. This is the value predicted for the lamellar domain spacing in strongly stretched chains in the bulk [31], which might be expected given the similarity between a vesicle bilayer, particularly at larger vesicle radii, and a bulk lamellar phase. An exponent of $2/3$ has also been observed [15] in experiments on vesicles formed of less strongly asymmetric copolymers. However, it is not in agreement with the experiments on highly asymmetric polymers of relevance here [12], where an exponent of 0.79 is observed.

Fig. 7 shows the predictions of the bilayer model for the same parameters. Here, most of the curves can be well approximated by power laws, with the exponent being close to the experimental value of 0.79 [12]. The exception is the shortest set of polymers ($N_A = 100$), where the vesicle is at the limit of being stable, only forming, as was noted earlier in this article and in [13], for a very narrow range of N_B. Even in this case, however, the curves for the larger values of the Flory-Huggins parameter ($\chi = 2, 2.5$ and 3) are close to power law $T_m \propto N_B^{0.79}$ for lower values of N_B, deviating as N_B approaches the value where the vesicle becomes unstable.

Discussion

By developing a mean-field model of vesicle formation in which the inner region of the vesicle membrane is composed of a single layer of interdigitated hydrophobic blocks, we have shown that the formation of vesicles of a preferred size for highly asymmetric copolymers is a robust prediction of mean-field models and does not depend on the assumption made in our earlier work [13] that the vesicle membrane is composed of two distinct layers of copolymers. Although the basic phenomenology of the two models is similar, it was shown that the model with interdigitation predicts that the vesicles should remain stable over a wider range of parameters than the bilayer model. The interdigitated model also predicts that the vesicle radius will be a less rapidly growing function of N_B than does the bilayer model, in arguably better agreement with experiments. However, the predictions of the bilayer model for the growth of the vesicle membrane thickness T_m are clearly better than those of the interdigitated model and are consistent with the experimental result of $T_M \propto N_B^{0.79}$ over a wide range of parameters. A possible explanation for this, advanced in [15], is that the structure of vesicle membranes lies between the extreme cases considered here and the central hydrophobic layer is neither completely segregated into two layers nor perfectly interdigitated.

Both models share the shortcoming of not predicting the experimental observation of the thickening of the vesicle membrane at almost constant overall vesicle radius as N_B is increased. A natural way of attempting to resolve this would be to model the system using self-consistent field theory (SCFT) [26]. Since SCFT and models of the kind studied here can agree well [32] for the self-assembly of micelles, the parameters from the current study could be used as starting values in the SCFT calculations. SCFT has been used to model a range of related systems, such as polymer brushes [33], bilayers [34] and micelles [35] and would provide a more detailed model of the system, with, for example, the interfaces no longer assumed to be perfectly sharp. It would also allow different interaction strengths between the various species in the system to be included, thereby relaxing the current assumption that the solvent consists of monomers of the same chemical composition as the hydrophilic blocks of the copolymers. Such a model would identify regions where vesicles of a preferred size are likely to form and allow this morphology to be targeted in experiments.

Acknowledgements

HJM gratefully acknowledges the support of a bursary from the University of Lincoln's Undergraduate Research Opportunities Scheme (UROS).

Declaration of interest statement

The authors declare no conflict of interest.

References

[1] Hamley IW. Block Copolymers in Solution: Fundamentals and Applications. Chichester (UK): Wiley; 2005.

[2] Jia L, Wang R, Fan Y. Encapsulation and release of drug nanoparticles in functional polymeric vesicles. Soft Matter 2020;16:3088–3095.

[3] Brannan AK, Bates FS. ABCA Tetrablock Copolymer Vesicles. Macromolecules 2004;37:8816–8819.

[4] Simons BD and Cates ME. Vesicles and onion phases in dilute surfactant solutions. J. Phys. II France 1992;2:1439–1451.

[5] Coldren BA, Warriner H, van Zanten R, et al. Zero Spontaneous Curvature and Its Effects on Lamellar Phase Morphology and Vesicle Size Distribution. Langmuir 2006;22:2474–2481.

[6] Enders S, Häntzschel D. Thermodynamics of aqueous carbohydrate surfactant solutions. Fluid Phase Equilib. 1998;153:1–21.

[7] Li W, Li H, Li J, et al. Self-assembled supramolecular nano vesicles for safe and highly efficient gene delivery to solid tumors. Int. J. Nanomedicine 2012;7:4661–4677.

[8] Morse DC and Milner ST. Statistical mechanics of close fluid membranes. Phys. Rev. E 1995;52:5918–5945.

[9] Storslett KJ and Muller SJ. Evaluation and comparison of two microfluidic size separation strategies for vesicle suspensions. Biomicrofluidics 2017;11:034112.

[10] Howse JR, Jones RAL, Battaglia G, et al. Templated formation of giant polymer vesicles with controlled size distributions. Nat. Mater. 2009;8:507–511.

[11] Safran SA, Pincus P, Andelman D. Theory of Spontaneous Vesicle Formation in Surfactant Mixtures. Science 1990;248:354–356.

[12] Warren NJ, Mykhaylyk OO, Ryan AJ, et al. Testing the Vesicular Morphology to Destruction: Birth and Death of Diblock Copolymer Vesicles Prepared via Polymerization-Induced Self-Assembly. J. Am. Chem. Soc. 2014;137:1929–1937.

[13] Greenall MJ. Size selection and stability of thick-walled vesicles. Phys. Chem. Liquids 2018;56:281–289.

[14] Discher DE, Eisenberg A. Polymer Vesicles. Science 2002;297:967–973.

[15] Battaglia G, Ryan AJ. Bilayers and Interdigitation in Block Copolymer Vesicles. J. Am. Chem. Soc. 2005;172:8757–8764.

[16] Kowalik M, Schantz AB, Naqi A, et al. Chemically specific coarse-grained models to investigate the structure of biomimetic membranes. RSC Adv. 2017;7:54756–54771.

[17] Leibler L, Orland H, Wheeler JC. Theory of critical micelle concentration for solutions of block copolymers. J. Chem. Phys. 1983;79:3550–3557.

[18] Noolandi J, Hong KM. Theory of Block Copolymer Micelles in Solution. Macromolecules 1983:16;1443–1448.

[19] Whitmore MD, Noolandi J. Theory of Micelle Formation in Block Copolymer-Homopolymer Blends. Macromolecules 1985:18;657–665.

[20] Mayes AM, Olvera de la Cruz M. Cylindrical versus Spherical Micelle Formation in Block Copolymer/Homopolymer Blends. Macromolecules 1988:21;2543–2547.

[21] Munch MR, Gast AP. Block Copolymers at Interfaces. 1. Micelle Formation. Macromolecules 1988:21;1360–1366.

[22] Roe RJ. Small-Angle X-ray Scattering Study of Micelle Formation in Mixtures of Butadiene Homopolymer and Styrene-Butadiene Block Copolymer. 3. Comparison with Theory. Macromolecules 1986:19;728–731.

[23] Lund R, Willner L, Linder P, et al. Structural Properties of Weakly Segregated PS-PB Block Copolymer Micelles in n-Alkanes: Solvent Entropy Effects. Macromolecules 2009:42;2686–2695.

[24] de Gennes PG. Conformations of Polymers Attached to an Interface. Macromolecules 1980:13;1069–1075.

[25] Milner S. Polymer Brushes. Science 1991:251;905–914

[26] Matsen MW. Self-Consistent Field Theory and Its Applications. In: Gompper G, Schick, M, editors. Soft Matter. Vol. 1, Polymer Melts and Mixtures. Weinheim: Wiley-VCH; 2006.

[27] Helfand E, Tagami Y. Theory of the Interface between Immiscible Polymers II. J. Chem. Phys. 1972:56;3592–3601.

[28] Roe R-J, Zin W-C. Determination of the Polymer-Polymer Interaction Parameter for the Polystyrene-Polybutadiene Pair. Macromolecules 1980:13;1221–1228.

[29] Press WH, Teukolsky SA, Vetterling WT, et al. Numerical Recipes. Cambridge (UK): Cambridge University Press; 2007.

[30] Ratcliffe LPD, Derry MJ, Ianiro A, et al. A Single Thermoresponsive Diblock Copolymer Can Form Spheres, Worms or Vesicles in Aqueous Solution. Angew. Chem. Int. Ed. 2019:58;18964–18970.

[31] Bates FS, Fredrickson GH. Block Copolymer Thermodynamics: Theory and Experiment. Annu. Rev. Phys. Chem. 1990:41:525–557.

[32] Greenall MJ, Buzza DMA, McLeish TCB. Micelle Formation in Block Copolymer/Homopolymer Blends: Comparison of Self-Consistent Field Theory with Experiment and Scaling Theory. Macromolecules 2009:42;5873–5880.

[33] Zhang PW, Shi, AC. Application of self-consistent field theory to self-assembled bilayer membranes. Chin. Phys. B 2015:24;128707.

[34] Ianiro A, Armes SP, Tuinier, R. Design principles for metamorphic block copolymer assemblies. Soft Matter 2020:16;2342-2349.

[35] Liaw CY, Henderson KJ, Burghardt WR, Wang J, Shull KR. Micellar Morphologies of Block Copolymer Solutions near the Sphere/Cylinder Transition 2015:48;173-183.

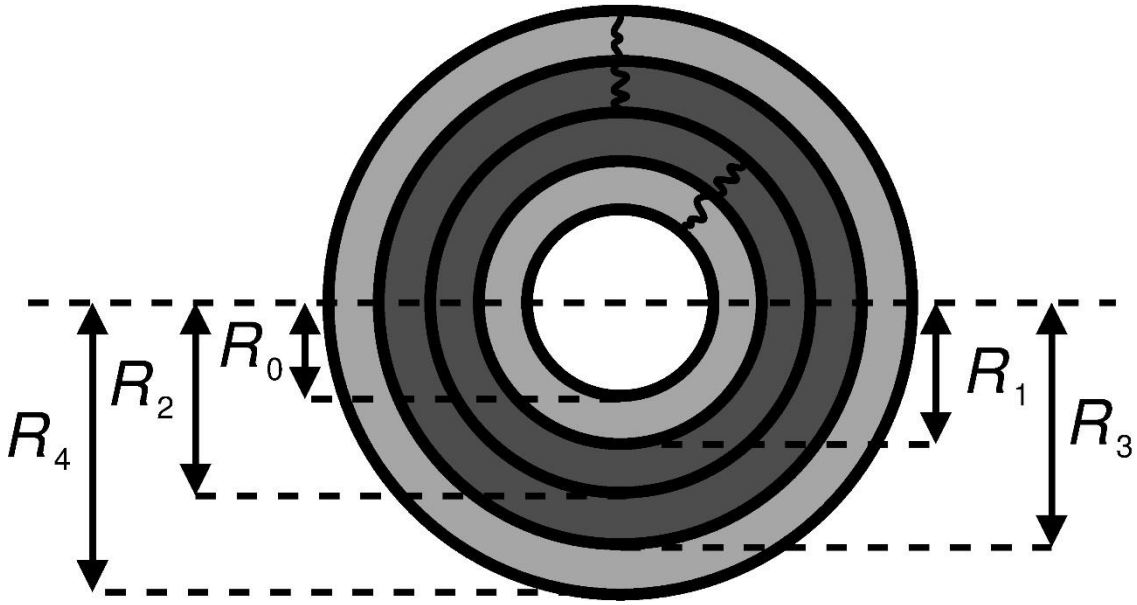

Figure 1. Cross-section of a spherical bilayer vesicle with outer radius R_4. The hydrophobic layers are shaded dark grey, and the hydrophilic layers are shaded light grey. The vesicle is surrounded by solvent and encloses a spherical volume of solvent with radius R_0. Two sample individual polymer molecules are shown. One of these lies in the inner layer and the other in the outer layer.

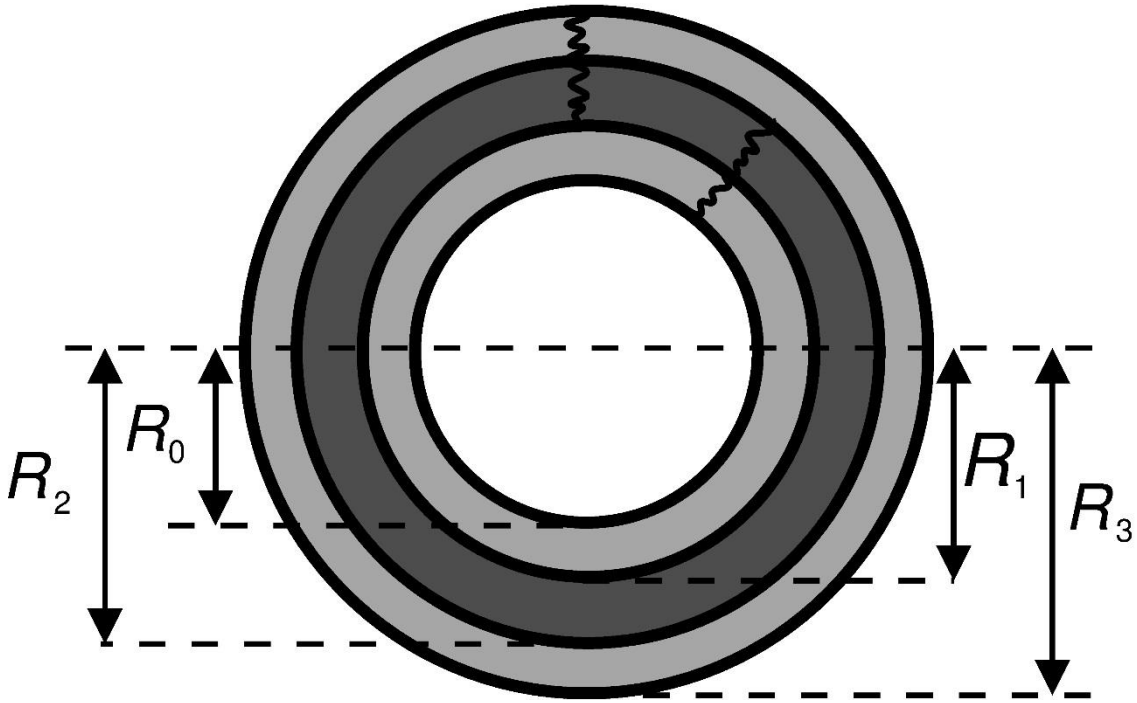

Figure 2. Cross-section of an interdigitated spherical vesicle with outer radius R_3. The central dark grey layer is hydrophobic, and the light grey layers are hydrophilic. As in Figure 1, the vesicle is surrounded by solvent and encapsulates a spherical volume of solvent with radius R_0. Two sample individual polymers are shown, one with its hydrophilic block in the inner layer and the other with its hydrophilic block in the outer layer.

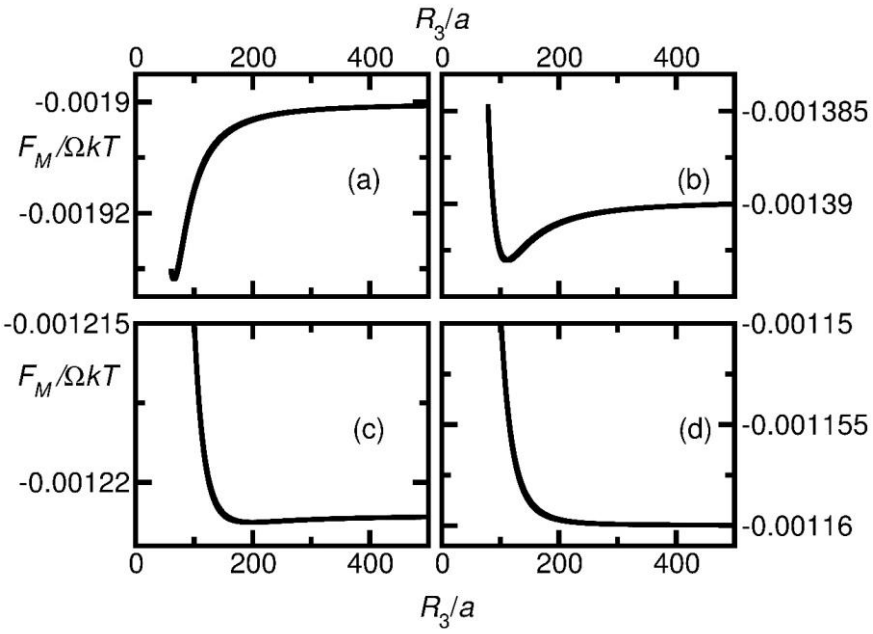

Figure 3. Total free energy of the system of vesicles versus the outer radius of the vesicle at fixed hydrophilic block length $N_A = 100$ and four different hydrophobic block lengths: (a) $N_B = 400$; (b) $N_B = 700$; (c) $N_B = 900$; (d) $N_B = 1000$.

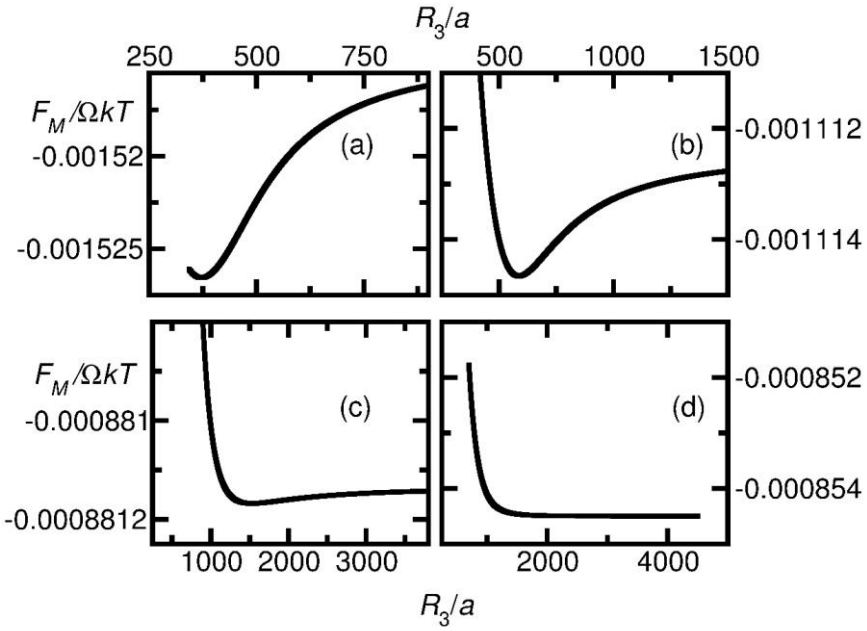

Figure 4. The total free energy of the system of vesicles as a function of the outer radius of the vesicle at fixed hydrophilic block length $N_A = 1000$ and four different hydrophobic block lengths: (a) $N_B = 7000$; (b) $N_B = 15000$; (c) $N_B = 29000$; (d) $N_B = 32000$.

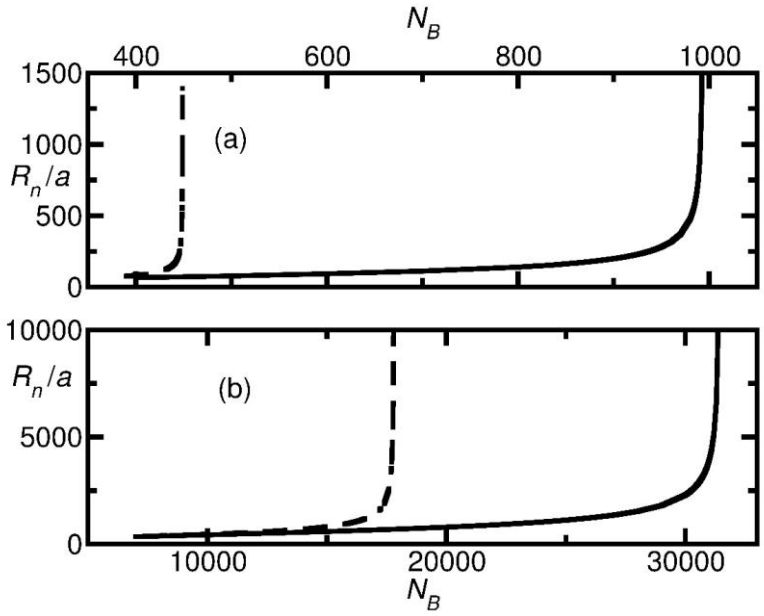

Figure 5. Outer radius of the vesicle versus the degree of polymerisation of the hydrophobic block for (a) $N_A = 100$ and (b) $N_A = 1000$. The full lines show the results for the interdigitated model (outer radius $R_n = R_3$) and the dashed lines those for the bilayer model (outer radius $R_n = R_4$).

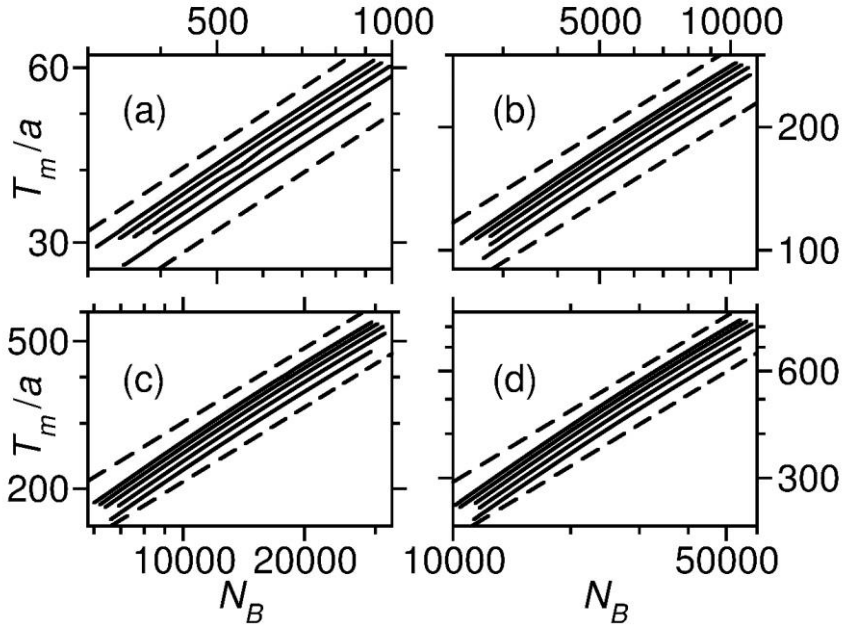

Figure 6. Membrane thickness in the interdigitated model $T_m = R_2 - R_1$ plotted against N_B for (a) $N_A = 100$; (b) $N_A = 500$; (c) $N_A = 1000$; (d) $N_A = 1500$. In each panel, the five curves correspond to $\chi = 1$ (lowest curve), $\chi = 1.5$, $\chi = 2$, $\chi = 2.5$ and $\chi = 3$ (highest curve). The dashed lines show power laws with an exponent of $2/3$.

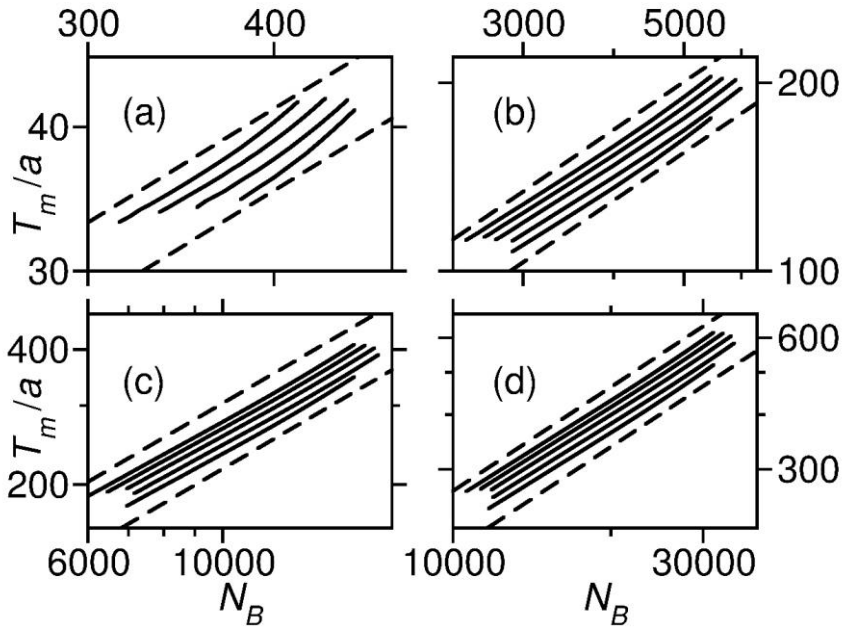

Figure 7. Membrane thickness in the bilayer model $T_m = R_3 - R_1$ plotted against N_B for (a) $N_A = 100$; (b) $N_A = 500$; (c) $N_A = 1000$; (d) $N_A = 1500$. In (b) to (d), the five curves correspond to $\chi = 1$ (lowest curve), $\chi = 1.5$, $\chi = 2$, $\chi = 2.5$ and $\chi = 3$ (highest curve). The dashed lines show power laws with an exponent of 0.79. In (a), the $\chi = 1$ curve is missing as the vesicle is not stable for this value.